Dynamic modelling and open-loop control of a two-degree-of-freedom twin-rotor multi-input multi-output system

S M Ahmad[1], **A J Chipperfield**[2] and **M O Tokhi**[3]*
[1]School of Engineering, The University of Manchester, Manchester, UK
[2]School of Engineering Sciences, University of Southampton, Southampton, UK
[3]Department of Automatic Control and Systems Engineering, The University of Sheffield, Sheffield, UK

Abstract: A dynamic model for the characterization of a two-degree-of-freedom (2DOF) twin-rotor multi-input multi-output system (TRMS) in hover is extracted using a black box system identification technique. Its behaviour in certain aspects resembles that of a helicopter, with a significant cross-coupling between longitudinal and lateral directional motions. Hence, it is an interesting identification and control problem. The extracted model is employed for designing and implementing a feedforward/open-loop control. Open-loop control is often the preliminary step for development of more complex feedback control laws. Hence, this paper also investigates open-loop control strategies using shaped command inputs for resonance suppression in the TRMS. Digital low-pass and band-stop shaped inputs are used on the TRMS test bed, based on the identified vibrational modes. A comparative performance study is carried out and the results presented. The low-pass filter is shown to exhibit better vibration reduction. When modal coupling exists, decoupled feedback controllers are incapable of eliminating vibration. In such cases, generating motion by shaped reference inputs is clearly advantageous.

Keywords: discrete-time systems, helicopter, linear identification, twin-rotor multi-input multi-output (MIMO) system, open-loop control, vibration suppression

NOTATION

a_i, b_i, c_i	unknown parameters to be identified
ARMAX	autoregressive moving average with exogenous input model
d.c.	direct current
$e(t)$	zero mean white noise
f	frequency (Hz)
F_1, F_2	thrust generated by the rotors in the vertical and horizontal planes respectively
$H(\mathrm{j}\omega)$	frequency response magnitude
L	tuning parameter of the elliptic filter
n_a, n_b, n_c	orders of the A, B and C polynomials of the ARMAX model
m	filter order
R_n	rational function
S_{xx} and S_{yy}	autospectral densities of the input and output signals respectively
S_{xy}	cross-spectral density between a pair of input and output signals
TRMS	twin-rotor multi-input multi-output system
$u_1(t)$	input to the main rotor (V)
$u_2(t)$	input to the tail rotor (V)
$y_1(t)$	pitch angle (rad)
$y_2(t)$	yaw angle (rad)
$\gamma^2_{xy}(f)$	ordinary coherence function
δ_1, δ_2	filter attenuation
ε	band edge value
λ	parameter controlling height of ripple in an elliptic filter
ω	radian frequency
ω_C	filter cut-off frequency
ω_p	pass-band edge frequency
ω_s	stop-band edge frequency

The MS was received on 6 October 2003 and was accepted after revision for publication on 10 June 2004.
* *Corresponding author: Department of Automatic Control and Systems Engineering, The University of Sheffield, Mappin Street, Sheffield, S1 3JD, UK. E-mail: o.tokhi@shef.ac.uk*

1 INTRODUCTION

The last decade has witnessed a phenomenal growth in numerous fields, including robotics, space structures and unconventional air vehicles. The significant features of these endeavours have included the introduction of innovative design, exotic structural materials and sophisticated control paradigms. This is a striking departure from the beaten paths of classical systems engineering philosophy. The focus of this paper, however, is restricted to the challenges and problems associated with flexible dynamic systems. Flexible structures, an area of intense interest in robotics [**1–3**] and spacecraft with flexible appendages [**4–6**] research, are attractive mainly because of their light weight and strength. In aerospace vehicles [**7, 8**] too, a flexible airframe is adopted owing to its light weight, thereby improving the thrust–weight ratio for a given power plant. The desirability of achieving a fast speed of response has prompted its use in systems such as flexible aircraft [**8**] and missiles [**9**]. This has inadvertently increased the modelling efforts significantly. Thus, such flexible vehicles/systems cannot be modelled by the rigid body assumption alone. For instance, Waszak and Schmidt [**10**] demonstrated the inadequacy of a rigid six degree-of-freedom (6DOF) description of the dynamics of a high-speed transport aircraft with a moderate level of structural flexibility. Consequently, the flight controller performance based on an inaccurate system model is palpable. Therefore, the need to account for aeroelastic effects will make modelling crucial for such vehicles.

The second important issue connected with a dynamic flexible plant is that of motion-induced vibration. Residual motion (vibration) is induced in flexible structures primarily as a result of faster motion commands. The occurrence of any vibration after the commanded position has been reached will require additional settling time before the new manoeuvre can be initiated. Therefore, in order to achieve a fast system response to command input signals, it is imperative to reduce this vibration. This feature is desirable in fast manoeuvring systems, such as fighter aircraft. Various approaches have been proposed to reduce vibration in flexible systems. They can be broadly categorized as open-loop (feedforward), closed-loop (feedback) or a combination of feedforward and feedback methods. Some prior work in vibration control is briefly reviewed.

Suk *et al.* [**5**] suggested and implemented torque-shaping approaches based on finite Fourier series expansion on a flexible space structure test bed (FSST). Another approach based on trigonometric series expansion is the work of Meckl and Seering [**11**] and references therein. A version of the approach using a pulse sequence expansion was suggested by Singer and Seering [**3**]. However, the simplest method for achieving the resonance suppression is via classical digital filters, such as Butterworth, elliptic and Chebyshev [**1, 2**].

The feedback or closed-loop approach utilizes measurements and estimates of the system states to reduce vibration. Dougherty *et al.* [**12**] and Franklin *et al.* [**13**] applied classical control to space structures in order to control the vibration and attitude (orientation). Recently, Teague *et al.* [**6**] developed a novel method for active control of the attitude and vibration of a flexible space structure using a global positioning system (GPS) as a sensor. Linear quadratic regulator (LQR) feedback was applied in this study.

However, a suitable strategy for controlling a system with resonant modes is to use a combination of feedback and feedforward. The role of a feedforward compensator is to place zeros near the lightly damped open-loop system poles, thereby creating *notches* at the corresponding resonant frequencies. The feedback loop, on the other hand, has a reduced task of controlling the rigid body movement alone. This combined approach is particularly widely employed in aircraft control design (see reference [**14**] and references therein).

The twin issue of modelling and control of a dynamic flexible system, manifested in an experimental test rig, representing a *complex* twin-rotor multi-input multi-output (MIMO) system (TRMS) (Fig. 1), is addressed in this paper. The TRMS, in addition to the rigid degrees of freedom, possesses elastic degrees of freedom, thereby compounding the modelling and control efforts. Further aspects of the TRMS are given in sections 2 and 3.

This paper will first briefly report the modelling aspects of a 2DOF TRMS—a detailed account can be found in the present authors' earlier work [**15**]. The second part will then utilize the modelling knowledge accrued in the first part to develop open-loop control strategies to attenuate system vibration. A shorter version of this work was presented at the IECON 2000 conference [**16**]. This work is a natural progression of the authors' investigation of a 1DOF modelling and control problem [**17**].

The paper presents a feedforward control technique that is related to a number of approaches known as 'input shaping control', discussed above. The goal of this input shaping control is to avoid excitation of the residual vibration at the end of the manoeuvre. The fundamental concept for this type of control is based on the well-established theory of digital filters. In these methodologies, a feedforward input signal is shaped so that it does not contain spectral components at the resonance eigenfrequencies of the system. The approach requires that the natural resonance frequencies of the system be determined through suitable identification and modelling techniques. Investigation of an MIMO open-loop control is a prelude to a future study of the development of more complex multivariable feedback control laws.

The paper is organized as follows. Sections 2 and 3 describe the underlying motivation and experimental rig set-up respectively. Section 4 briefly discusses modelling and presents the corresponding experimental results.

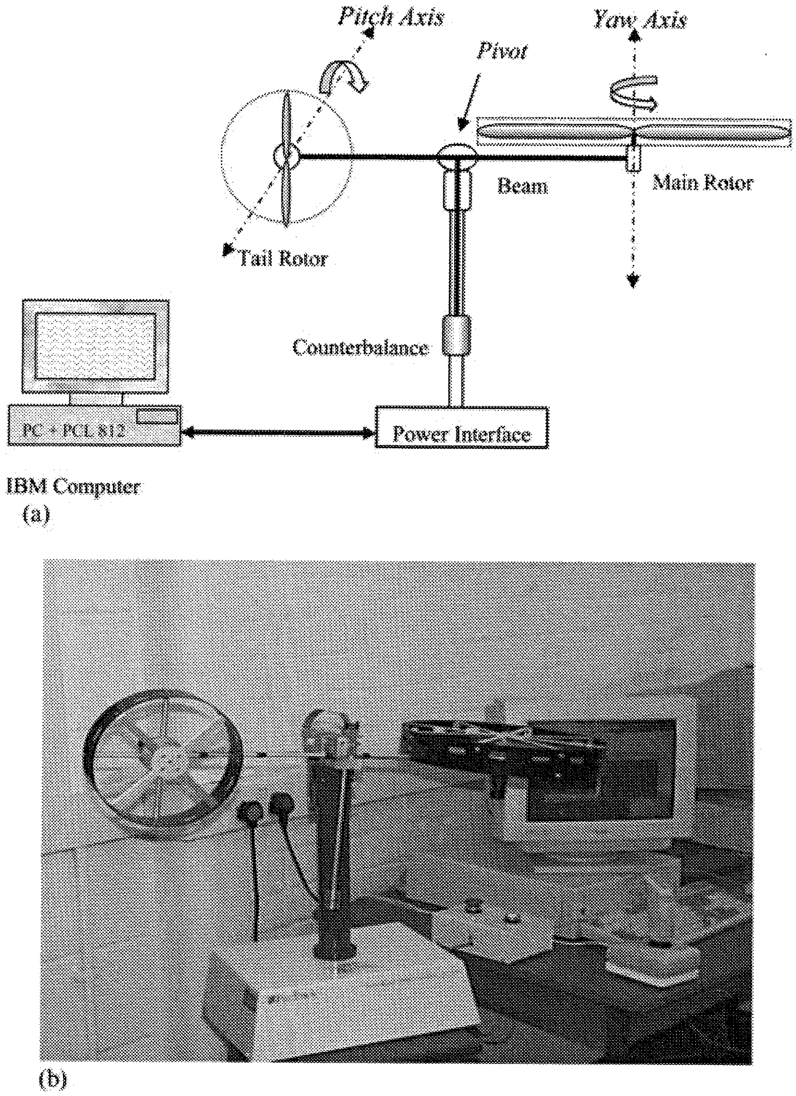

Fig. 1 (a) Twin-rotor MIMO system schematic diagram and (b) the TRMS in 'hover' mode

Section 5 addresses TRMS vibration mode analysis and control. Section 6 discusses filter design and implementation, and section 7 concludes the paper.

2 MOTIVATION

Although the TRMS shown in Fig. 1 does not fly, it has a striking similarity to a helicopter, such as system non-linearities and cross-coupled modes. The TRMS, therefore, can be perceived as an unconventional and complex 'air vehicle' with a flexible main body. These system characteristics present formidable challenges in modelling, control design and analysis. The TRMS is a laboratory set-up designed for control experiments by Feedback Instruments Limited [**18**]. The main differences between a helicopter and the TRMS are as follows:

1. In a single main rotor helicopter the pivot point is located at the main rotor head, whereas in the case of the TRMS the pivot point is mid-way between the two rotors.
2. In a helicopter, lift is generated via *collective pitch control*, i.e. pitch angles of all the blades of the main rotor are changed by an identical amount at every point in azimuth, but at a constant rotor speed. However, in the case of the TRMS, pitch angles of all the blades are fixed and speed control of the main rotor is employed to achieve vertical control.
3. Similarly, yaw is controlled in a helicopter by changing, by the same amount, the pitch angle of all the blades of the tail rotor. In the TRMS, yawing is effected by varying the tail rotor speed.
4. There are no *cyclical controls* in the TRMS, whereas *cyclic* is used for directional control in a helicopter.

However, like a helicopter, there is a strong cross-coupling between the collective (main) rotor and the tail rotor.

Although the TRMS rig reference point is fixed, it still resembles a helicopter by being highly non-linear with strongly coupled modes. Such a plant is thus a good benchmark problem to test and explore modern identification and control methodologies. The experimental set-up simulates similar problems and challenges encountered in real systems. These include complex dynamics leading to both parametric and dynamic uncertainty, unmeasurable states, sensor and actuator noise, saturation and quantization, bandwidth limitations and delays.

The presence of flexible dynamics in the TRMS is an additional motivating factor for this research. There is an immense interest in design, development, modelling and control of flexible systems owing to its utility in a multitude of applications, for example in aerospace and robotics.

3 EXPERIMENTAL SET-UP

The TRMS considered in this work is described in Fig. 1. This consists of a beam pivoted on its base in such a way that it can rotate freely both in its horizontal and vertical planes. There are rotors (the main and tail rotors), driven by d.c. motors, at either end of the beam. A counterbalance arm with a weight at its end is fixed to the beam at the pivot. The state of the beam is described by four process variables: yaw and pitch angles measured by position sensors fitted at the pivot, and two corresponding angular velocities. Two additional state variables are the angular velocities of the rotors, measured by tachogenerators coupled with the driving d.c. motors.

In a typical helicopter, the aerodynamic force is controlled by changing the angle of attack of the blades. The laboratory set-up is constructed such that the angle of attack of its blades is fixed, and the aerodynamic force is controlled by varying the speed of the motors. Therefore, the control inputs are supply voltages of the d.c. motors. A change in the voltage value results in a change in the rotational speed of the propeller, which results in a change in the corresponding angle (in radians) of the beam **[18]**. The main rotor produces a lifting force allowing the beam to rise vertically (pitch angle/movement), while the tail rotor, smaller than the main rotor, is used to make the beam turn left or right (yaw angle/movement).

Aerodynamic modelling of air vehicles is generally carried out either by employing a wind tunnel or by using flight test measurements. In the former approach, static and dynamic tests are carried out on a scale model of the actual aircraft to obtain important aerodynamic derivatives. Important force–velocity and moment–velocity derivatives are estimated utilizing the six-component force and moment balance. In the latter approach, on the other hand, modelling is accomplished by flying the air vehicle and subjecting it to different test signals to excite the system modes. Since carrying out flight tests on a full-scale vehicle is prohibitively expensive and difficult, wind tunnel or laboratory-scale tests like the ones described here are far more attractive.

4 SYSTEM MODELLING

The objective of the identification experiments is to estimate a linear time-invariant (LTI) model of the 2DOF TRMS in hover (see Fig. 1b) without any prior system knowledge pertaining to the exact mathematical model structure, i.e. black box modelling.

It is intuitively assumed that the rigid body resonance modes of the TRMS lie in a low frequency range of 0–1 Hz, while the main rotor dynamics are at significantly higher frequencies. The rig configuration is such that it permits open-loop system identification, unlike a helicopter which is open-loop unstable in hover mode. In Fig. 2, the input signals u_1 and u_2 represent voltage inputs to the main rotor and tail rotor respectively. The outputs y_1 and y_2 represent pitch and yaw angles in radians respectively. Strong coupling exists between the two channels, and this may be accounted for by representing the dynamics of the TRMS by the multivariable transfer function model given in Fig. 2.

System identification is carried out using a pseudo-random binary sequence (PRBS) signal of 2 Hz bandwidth. The duration of the test signal was 120 s, and a sampling interval of 10 Hz was chosen by trial and error. The details of MIMO system identification of the TRMS can be found in previous work by the present authors **[15]**. In this study, however, results will be presented briefly.

Strong interaction was observed among channels $u_1 \rightarrow y_1$, $u_1 \rightarrow y_2$ and $u_2 \rightarrow y_2$ but not between $u_2 \rightarrow y_1$ during the experimentation. These couplings between various channels were confirmed by coherence spectra **[15]**. Since no correlation exists between $u_2 \rightarrow y_1$, this channel was not investigated for model fitting.

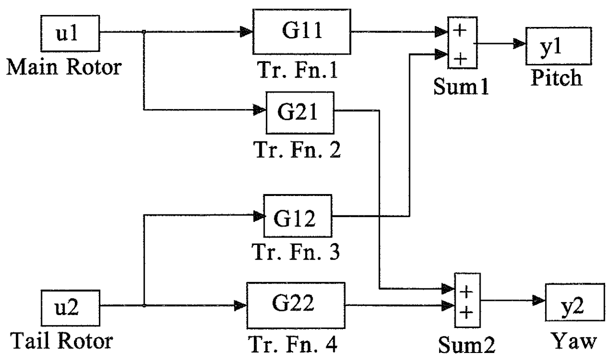

Fig. 2 MIMO transfer function model

4.1 Coupling analysis for a 2DOF TRMS

The two modes of operation of the TRMS, i.e. rotation in the vertical plane (pitch) and rotation in the horizontal plane (yaw), exhibit strong modal coupling. This coupling directly influences the velocities of the TRMS in both planes. The cross-coupling through the $u_1 \rightarrow y_2$ channel exists in the frequency range of interest, i.e. 0–1 Hz, and is evident from the coherence spectrum of Fig. 3. The coherence function $\gamma_{xy}^2(f)$ is given by

$$\gamma_{xy}^2(f) = \frac{|S_{xy}(f)|^2}{S_{xx}(f)S_{yy}(f)} \quad (1)$$

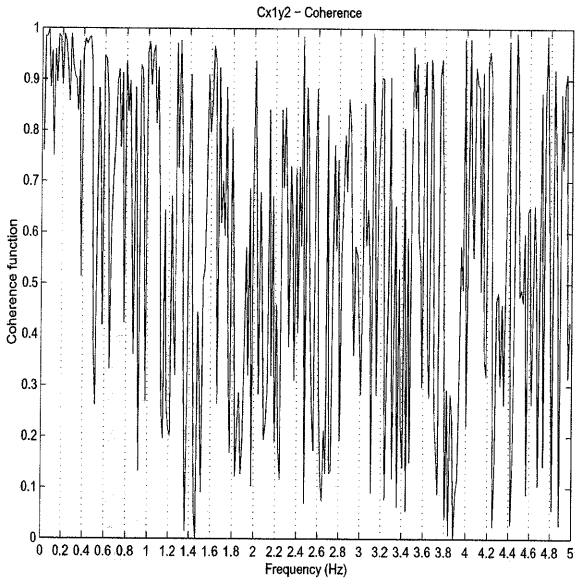

Fig. 3 Coherence spectrum, $u_1 \rightarrow y_2$ channel

where S_{xx} and S_{yy} are the autospectral densities of the input and output signals respectively and S_{xy} is the cross-spectral density between the input and output signals. By definition, the coherence function lies between 0 and 1 for all frequencies f:

$$0 \leqslant \gamma_{xy}^2(f) \leqslant 1$$

If $x(t)$ and $y(t)$ are completely unrelated, the coherence function will be zero. Thus, coherence of 1 indicates (coupled) a linear relationship between the two signals, and, if the coherence function is equal to zero, it implies that the two signals are completely unrelated.

The implication of this coupling is that if motion in one direction contains energy at frequencies corresponding to mode shapes in another direction, then that motion will produce vibration in the other direction and could lead to instability. Hence, accurate identification and subsequent processing of these modes is important from a systems engineering perspective.

4.2 Mode or structure determination

Theoretically, the TRMS will have an infinite number of resonance modes with associated frequencies. However, it is intuitively assumed that the main dynamics (modes) of the TRMS lie in the 0–1 Hz range. It is further assumed that the rotor dynamics are at significantly higher frequencies than the rigid body modes. Investigations are carried out, under these broad hypotheses, to characterize the behaviour of the TRMS.

The power spectral density plot of the pitch (y_1) and the yaw (y_2) responses (see Fig. 4) to the PRBS input signal u_1, indicates closely spaced modes between 0 and

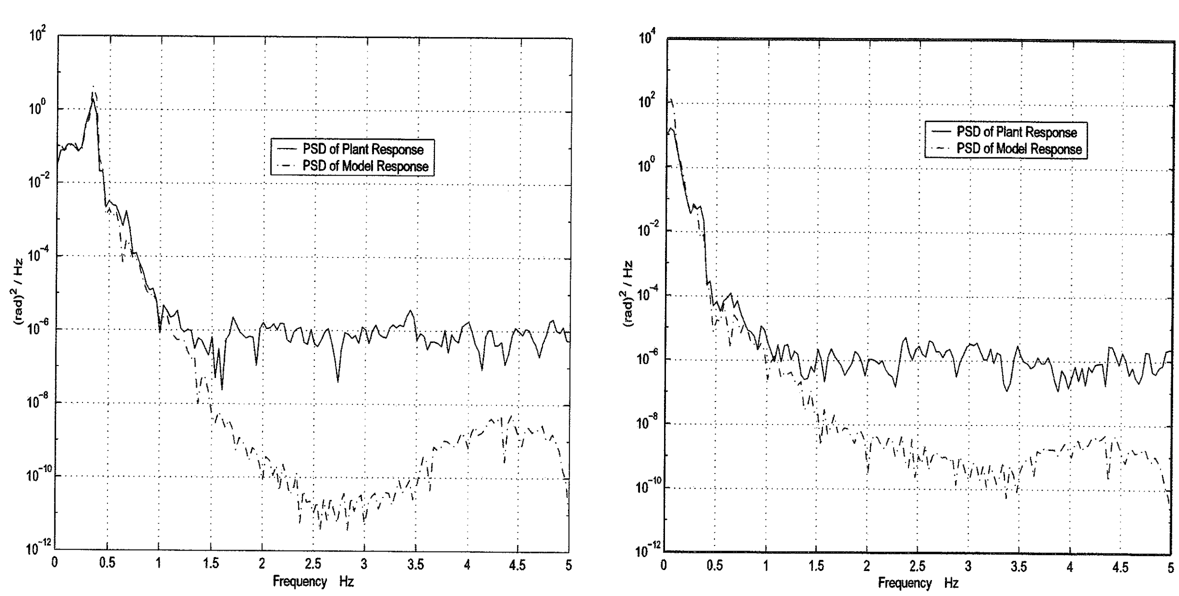

Fig. 4 Power spectral density: (a) pitch response, $u_1 \rightarrow y_1$; (b) yaw response, $u_1 \rightarrow y_2$

1 Hz, as expected. The pitch channel $u_1 \rightarrow y_1$ has a main resonant mode at 0.34 Hz, and the yaw channel $u_1 \rightarrow y_2$ at around 0.1 Hz. Hence, a model order of 2 or 4 corresponding to dominant modes for each channel is anticipated.

Similarly, for the second input u_2 and second output y_2, a model order of 2 or 4 is expected, corresponding to the mode at 0.1 Hz, and a rigid body (i.e. zero resonance frequency) yaw mode (see Fig. 5). The results of identification are summarized in Table 1.

4.3 Parametric modelling

From the authors' earlier work [**15**], an autoregressive moving average with exogenous input (ARMAX) model structure was found best to characterize the system dynamics. The ARMAX model is represented as

$$\begin{aligned} y(t) + a_1 y(t-1) + \cdots + a_{n_a} y(t-n_a) \\ = b_1 u(t-1) + \cdots + b_{n_b} u(t-n_b) \\ + e(t) + c_1 e(t-1) + \cdots + c_{n_c} e(t-n_c) \end{aligned} \quad (2)$$

where a_i, b_i and c_i are the parameters to be identified, and $e(t)$ is the zero mean white noise. This structure takes into account both the true system and noise models.

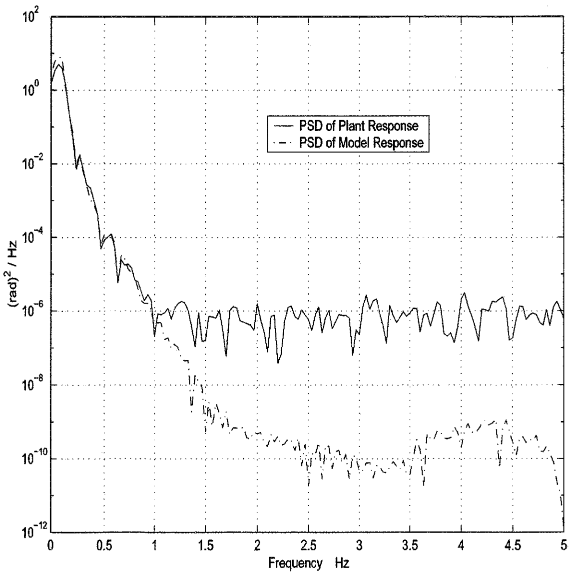

Yaw response, *u2 → y2*.

Fig. 5 Power spectral density, yaw response, $u_2 \rightarrow y_2$

Table 1 Identified natural frequencies

DOF	Channel	Identified system modes (Hz)
2DOF	$u_1 \rightarrow y_1$	0.1 and 0.34
	$u_1 \rightarrow y_2$	0.1
	$u_2 \rightarrow y_2$	0.1
	$u_2 \rightarrow y_1$	No cross coupling

Power spectral density plots of the plant and the model outputs are superimposed in Figs 4 and 5. It is observed that the dominant modes of the models and the plant coincide quite well, implying good model predicting capability of the important system dynamics. Thus, it is assumed that the identified models are fairly accurate and suitable for open- and/or closed-loop controller design.

5 TRMS VIBRATION MODE ANALYSIS

In general, for flexible structures/aircraft, the parameter that has an influence on the flexible modes is the mass distribution, which may change the frequencies of the modes and the accuracy of the model. In the case of an aircraft, the speed and Mach number also have an influence on the modes of the system. This is relevant to the TRMS, which can be interpreted as a centrally supported cantilever beam with loads (rotors) at both ends. The non-uniform mass distribution due to the rotors and the rotor torque at normal operating conditions are the main causes of beam deflection. The deflection of the beam is due to the excitation of the *resonance modes* by an input signal that is rich in system eigenfrequencies. The different deflection profiles of the beam, occurring at corresponding resonance frequencies, represent the *normal mode shapes* of the system. Thus, in theory, the beam will have an infinite number of such normal modes with associated mode shapes and frequencies.

In conventional resonance, a dynamic system is excited by a fluctuating input, the frequency of which is equal to the natural frequency of the dynamic system. The TRMS could oscillate and become unstable if its natural frequency of oscillation is close to or within the frequency range of the disturbance/excitation due to the rotor. A system or a structure will oscillate, and could become unstable, owing to the excitation of the resonance modes by an input signal or disturbance that is rich in system eigenfrequencies. Hence, accurate identification and subsequent processing of these modes is important from a systems engineering perspective. In particular, this is important for designing control laws to ensure that structural component limits and fatigue loads are not exceeded for the full operating range of aircraft/TRMS manoeuvres. Moreover, this will be useful for minimizing structural damage via resonant mode suppression, reduction in pilot workload and passenger comfort in the case of an aircraft. Similar advantages will result for other systems with elastic modes.

5.1 Open-loop control

The presence of elastic modes, as evident from the results in section 3 and summarized in Table 1, are the primary cause of residual vibration in the TRMS. Various approaches have been proposed to reduce vibration in flexible systems. These broadly include feedforward, feedback or a combination of feedforward and feedback methods. The feedback control paradigm for 1DOF has been investigated and reported by the present authors in recent work [**19**].

In the present study, however, open-loop control methods are considered for vibration control, where the control input is developed by considering the physical and vibrational property of the flexible system. The goal of this research is to develop methods to reduce motion and uneven mass-induced vibrations in the TRMS during operation. The assumption is that the motion and the rotor load are the main sources of system vibration. Thus, input profiles that do not contain energy at system natural frequencies do not excite structural vibration and hence require no additional settling time. Digital filters are used for preprocessing the input to the plant, so that no energy is ever put into the system near its resonance. The advantage of employing shaped reference inputs when modal coupling exists, as is the case with the TRMS, would be evident from the results.

5.2 Digital filters for command shaping

In order to filter out the input energy at the system natural frequencies, two different mechanisms can be adopted. The first approach is to pass the command signal through a low-pass filter. This will attenuate input energy at all frequencies above the filter cut-off frequency. An important consideration is to achieve a steep roll-off rate at the cut-off frequency so that the input energy can be passed for frequencies close to the lowest natural frequency of the TRMS. Another approach that can be employed to attenuate input energy at plant natural frequencies is to use band-stop filters with centre frequencies at selected significant resonance modes of the TRMS.

Different types of filter, such as Butterworth, elliptic and Chebyshev filters, can be used. In this study, it is mainly the Butterworth type that is employed because of its simple design and in particular as its pass band and stop band are without ripples. The elliptic-type filter is also employed as a band-stop filter in the latter part of this work, primarily because it has a short transition region from pass band to stop band.

The Butterworth filter is called the *maximally flat filter* because of lack of ripple in the pass band. However, the Butterworth filter achieves its flatness at the expense of a relatively wide transition region. The Butterworth filter is defined by the squared magnitude transfer function [**20**]

$$|H_{\mathrm{B}}(\mathrm{j}\omega)|^2 = \frac{1}{1+(\omega/\omega_{\mathrm{C}})^{2m}} = \frac{1}{1+\varepsilon(\omega/\omega_{\mathrm{p}})^{2m}} \qquad (3)$$

where m is the order of the filter, ω_{C} is the filter cut-off frequency, ω_{p} is the pass-band edge frequency and $(1+\varepsilon^2)^{-1}$ is the band edge value of $|H_{\mathrm{B}}(\mathrm{j}\omega)|^2$. Thus, from the above equation the filter order that is needed to achieve attenuation δ_2 at a particular frequency is easily obtained as

$$m = \frac{\log(1/\delta_2^2 - 1)}{2\log(\omega_{\mathrm{s}}/\omega_{\mathrm{p}})} = \frac{\log(\delta_1/\varepsilon)}{\log(\omega_{\mathrm{s}}/\omega_{\mathrm{p}})} \qquad (4)$$

where, by definition, $\delta_2 = (1+\delta_1^2)^{-0.5}$. Therefore, the Butterworth filter is completely described by the parameters δ_2, m, ε and the ratio $\omega_{\mathrm{s}}/\omega_{\mathrm{p}}$. This equation can be utilized with arbitrary δ_1, δ_2, ω_{C} and ω_{s} to yield the desired filter order m from which filter design is easily obtained.

The elliptic filter has the shortest transition region from pass band to stop band of any filter with the same order and ripple heights. The elliptic design is optimum in this sense. Therefore, the elliptic filter is ideal for applications where ripples can be tolerated and short transition regions are demanded. The squared magnitude transfer function of the elliptic filter is given as

$$|H_{\mathrm{E}}(\mathrm{j}\omega)|^2 = \frac{1}{1+\lambda^2[R_n(\omega/\omega_{\mathrm{C}}, L)]^2} \qquad (5)$$

where the parameter λ controls the height of the ripples, ω_{C} controls the frequency breakpoint, R_n is a rational function, and the parameter L controls the width of the transition region, the ripple height in the stop band, and interacts with ω_{C} to affect the breakpoint [**21**].

The design of elliptic filters is much more complex than that of the Butterworth and Chebyshev types. This is because the designer must select the order of the filter, the cut-off frequency and the parameter L. The design is further complicated because ω_{C} and L interact in determining the breakpoint of the filter. For this reason, elliptic filters are designed via design tables, given in most standard textbooks [**22**].

The open-loop control experiments are conducted for a 2DOF TRMS, allowing movement in both the horizontal and vertical planes. Note that the significant modes of the TRMS identified in section 3 that need attenuation are given in Table 1 for the 2DOF plant. Analogous to modelling, the sampling interval of 10 Hz is used for 2DOF control experiments. The TRMS operating point is the flat horizontal position of the beam.

6 IMPLEMENTATION AND RESULTS

To study system performance, initially an unshaped doublet input shown in Fig. 6 is used to drive the main rotor (u_1), and the corresponding system responses y_1 and y_2 are measured (see the solid lines in Figs 7 and 8). The response overshoots and shows considerable

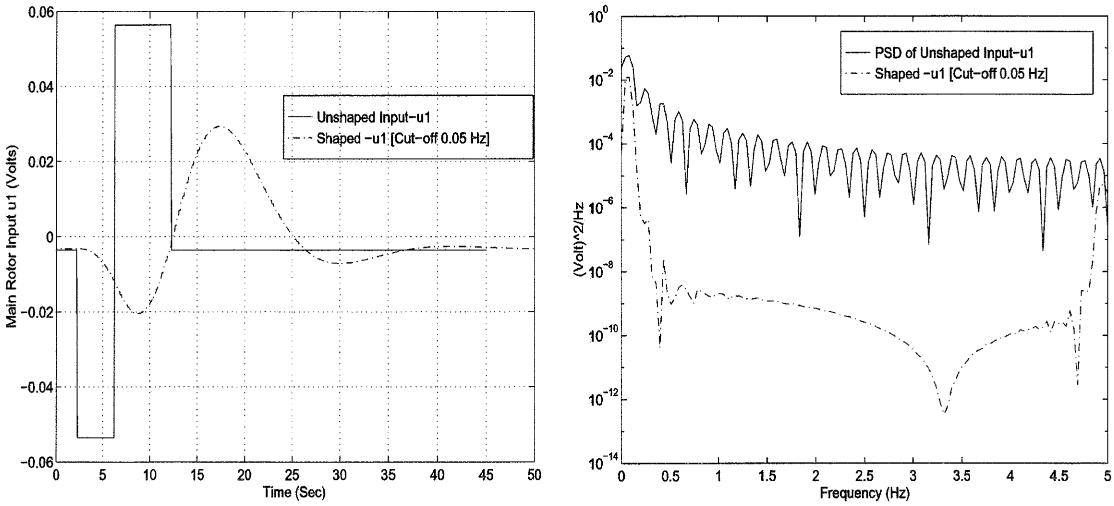

(a) Time domain. (b) Power spectral density.

Fig. 6 Doublet input using a low-pass filter: (a) time domain; (b) power spectral density

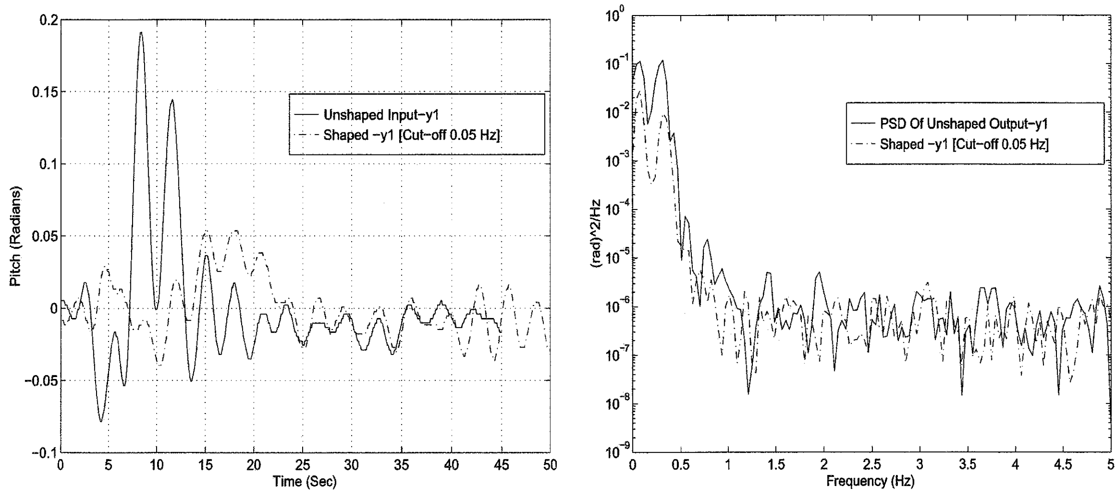

(a) Time domain. (b) Power spectral density.

Fig. 7 Pitch response to a low-pass filtered doublet input, $u_1 \rightarrow y_1$: (a) time domain; (b) power spectral density

residual vibration, with dominating modes at 0.1 and 0.31 Hz. The procedure is then repeated, exciting the tail rotor (u_2), using the same input as above. The response y_2 is shown in Fig. 9 by solid lines. Even here the response overshoots, but with mild residual vibration. The dominant mode in this axis lies at 0.1 Hz. The main objective of this section is to suppress the system vibrations at the first few dominant resonance modes in both axes simultaneously. Two different types of strategy can be adopted to filter out the input energy at the natural frequencies. The first approach is to pass the input through a low-pass filter. This will attenuate input energy at all frequencies above the cut-off frequency. An alternative approach is to remove energy at the system natural frequencies by employing narrow-band band-stop filters, with centre frequencies selected at dominant resonance modes of the system. In the present work, both these methods are investigated, employing low-pass Butterworth and band-stop elliptic filters. Finally, Table 2 summarizes the results of the open-loop control experiments.

6.1 Low-pass shaped input

A third-order low-pass Butterworth filter with a cut-off frequency at 0.05 Hz was designed and employed for off-line processing of the doublet input. The motive behind selecting the cut-off frequency at 0.05 Hz lies in the fact that the lowest vibrational mode of the system is found to be at 0.1 Hz. Hence, to attenuate resonance of the system, the cut-off frequency must be selected lower than the lowest vibrational mode. The shaped doublet input is then injected in the main rotor (u_1) of the TRMS, and

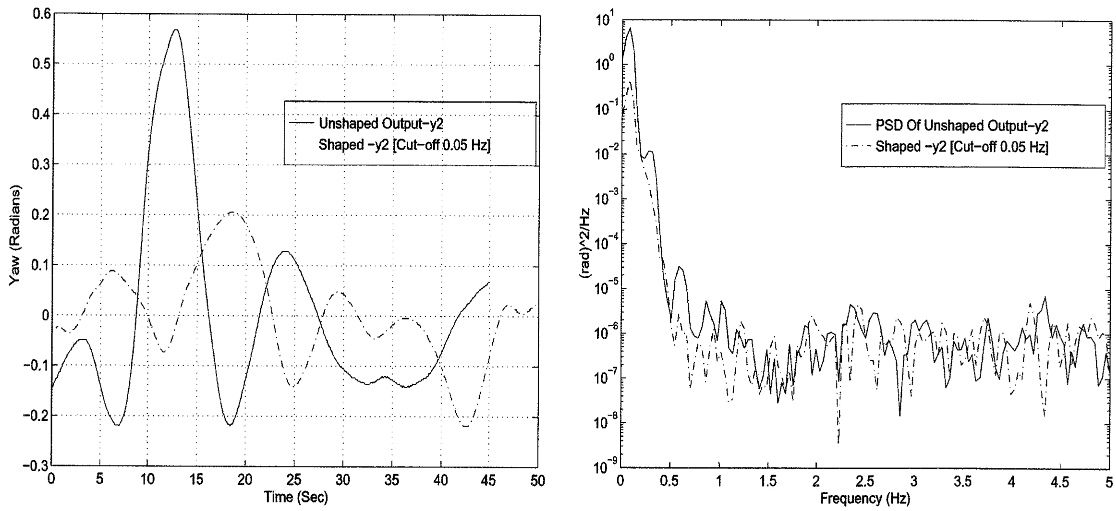

(a) Time domain. (b) Power spectral density.

Fig. 8 Yaw response to a low-pass filtered doublet input, $u_1 \rightarrow y_2$: (a) time domain; (b) power spectral density

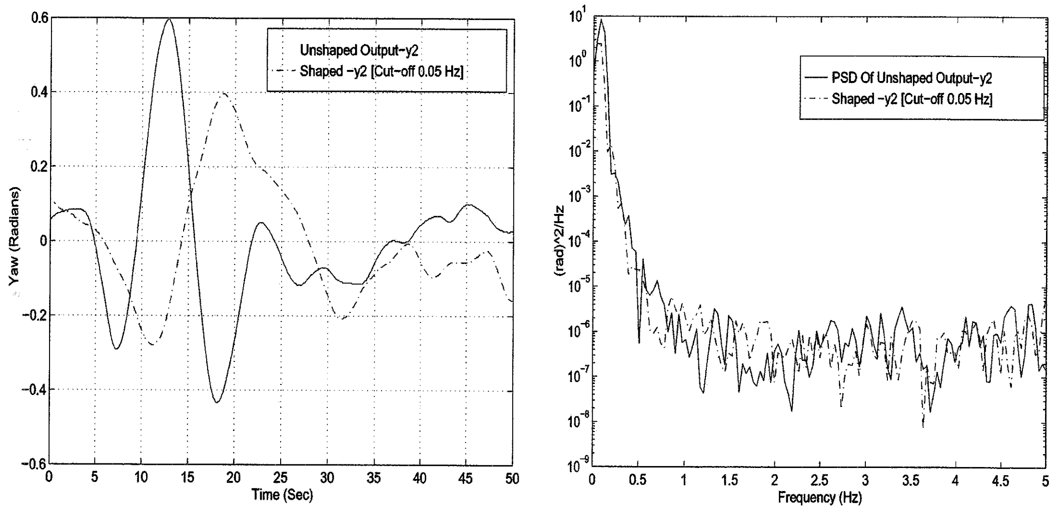

(a) Time domain. (b) Power spectral density.

Fig. 9 Yaw response to a low-pass filtered doublet input, $u_2 \rightarrow y_2$: (a) time domain; (b) power spectral density

Table 2 MIMO open-loop control: mode attenuation

		Filter 1 (0.25–0.4 Hz)	Filter 2 (0.01–0.15, 0.25–0.4 Hz)	Filter 3 (0.05–0.15 Hz)	Low-pass cut-off (0.05 Hz)
$u_1 \rightarrow y_1$	0.1		20 dB		10.45 dB
	0.34	13.98 dB	13.98 dB		20.91 dB
$u_1 \rightarrow y_2$	0.1		36.25 dB		24.22 dB
$u_2 \rightarrow y_2$	0.1			18.59 dB	10.63 dB

the pitch (y_1) and yaw (y_2) responses are measured. The low-pass Butterworth filtered doublet is shown in Fig. 6, and the corresponding pitch and yaw responses in Figs 7 and 8. It is noted that the attenuation in the level of vibration at the first and second resonance modes of the $u_1 \rightarrow y_1$ channel are 10.45 and 20.91 dB respectively, as shown in Fig. 7, with the shaped input in comparison with the unshaped doublet. An attenuation of 24.22 dB is achieved for the $u_1 \rightarrow y_2$ channel (see Fig. 8).

For the $u_2 \rightarrow y_2$ channel, a spectral attenuation of 10.63 dB is obtained using the shaped input, as is evident from Fig. 9. Note that the cut-off frequency of 0.05 Hz, which is very close to the rigid body motion dynamics, results in substantial attenuation of the input to the rigid body mode. This is reflected in the low-magnitude responses compared with the unshaped responses.

6.2 Band-stop shaped input

As before, a second-order digital elliptic filter was used to study the TRMS performance with a band-stop shaped input. For effective suppression of the vibrations of the system, the centre frequency of the band-stop filter has to be at exactly the same frequency or as close as possible to the resonance frequency. From Table 1 it is observed that the main resonant mode lies at 0.1 and 0.34 Hz for the $u_1 \rightarrow y_1$ channel and at 0.1 Hz for the $u_1 \rightarrow y_2$ and $u_2 \rightarrow y_2$ channels. Thus, three filters with different stop-band frequency ranges were investigated:

(a) 0.25–0.4 Hz
(b) 0.05–0.15 Hz and 0.25–0.4 Hz
(c) 0.05–0.15 Hz.

A band-stop shaped doublet input, shown in Fig. 10 by dotted and dashed lines, was used, and the responses were measured.

It can be seen from Fig. 11b that the dominating 0.34 Hz vibration mode has been reduced by almost 14 dB with the use of filter 1. The time history reveals

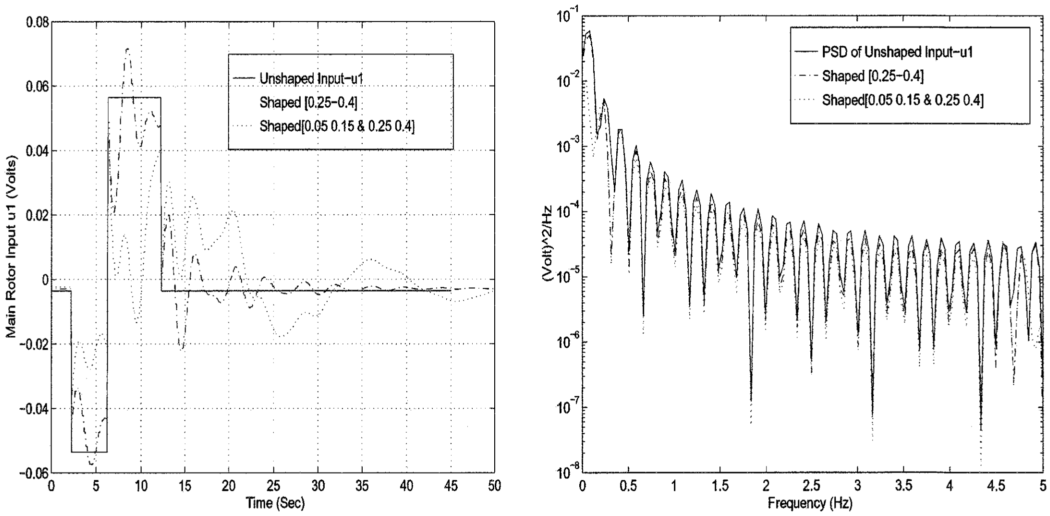

(a) Time domain. (b) Power spectral density.

Fig. 10 Doublet input using a band-stop filter: (a) time domain; (b) power spectral density

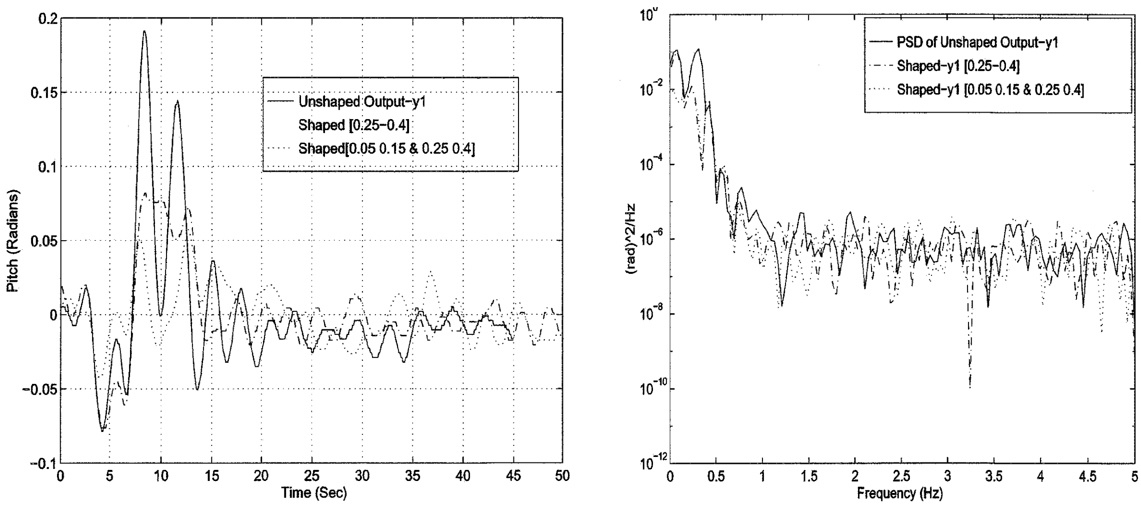

(a) Time domain. (b) Power spectral density.

Fig. 11 Pitch response with a band-stop filtered doublet input, $u_1 \rightarrow y_1$: (a) time domain; (b) power spectral density reasonable damping and residual vibration disappearing quickly. Obviously, this filter has no bearing on the $u_1 \rightarrow y_2$ channel. The shaped input has not lost much of its profile, and hence the response y_1 is fairly smooth. The intent in using this filter, i.e. just suppressing the 0.34 Hz mode, was to gauge the system performance and compare it with the performance of filter 2.

Filter 2 is designed to suppress prominent resonant modes appearing in both the channels. Some observations are noted for this filter:

1. The shaped input is badly distorted, and hence good tracking of the command is unlikely.
2. The time history of Figs 11 to 13 displays good damping (i.e. no overshoot) and minimal residual vibrations.
3. The response y_1 is not smooth, indicating inconsistent and attenuated kinetic energy supply to the system.
4. As in the case of a low-pass filter, a band-stop frequency very close to the rigid body mode results in significant deterioration in the output magnitude and shape.
5. It is noted that the spectral attenuation in the system vibration at the first (0.1 Hz) and second (0.34 Hz) mode is 20 and 13.98 dB respectively for the $u_1 \rightarrow y_1$ channel (Fig. 11) and 36.25 dB for the $u_1 \rightarrow y_2$ channel (Fig. 12).

Filter 3 was employed for the $u_2 \rightarrow y_2$ channel (Fig. 13) and resulted in a vibration reduction of 18.59 dB. The results of the MIMO open-loop experiments are summarized in Table 2.

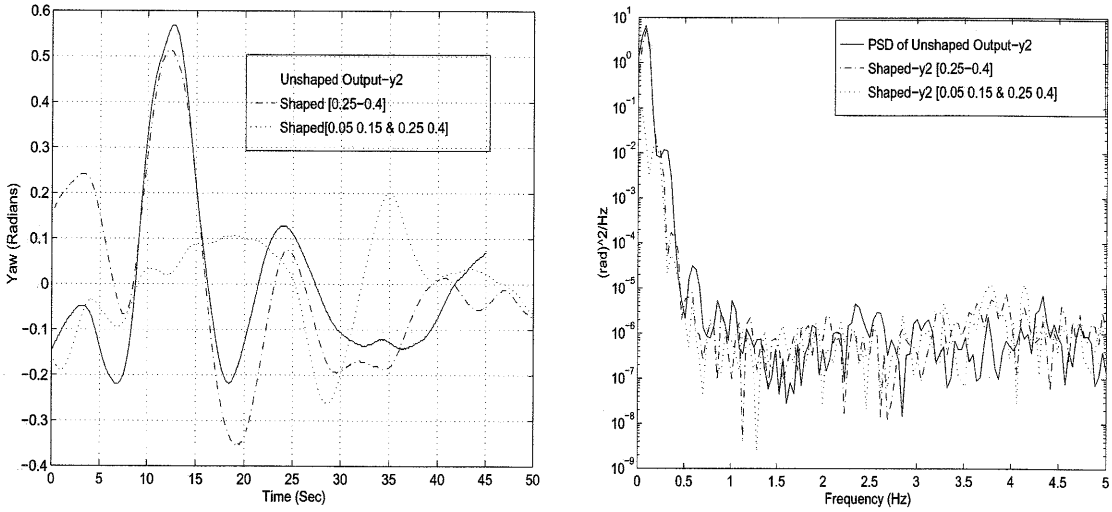

(a) Time domain. (b) Power spectral density.

Fig. 12 Yaw response with a band-stop filtered doublet input, $u_1 \rightarrow y_2$: (a) time domain; (b) power spectral density

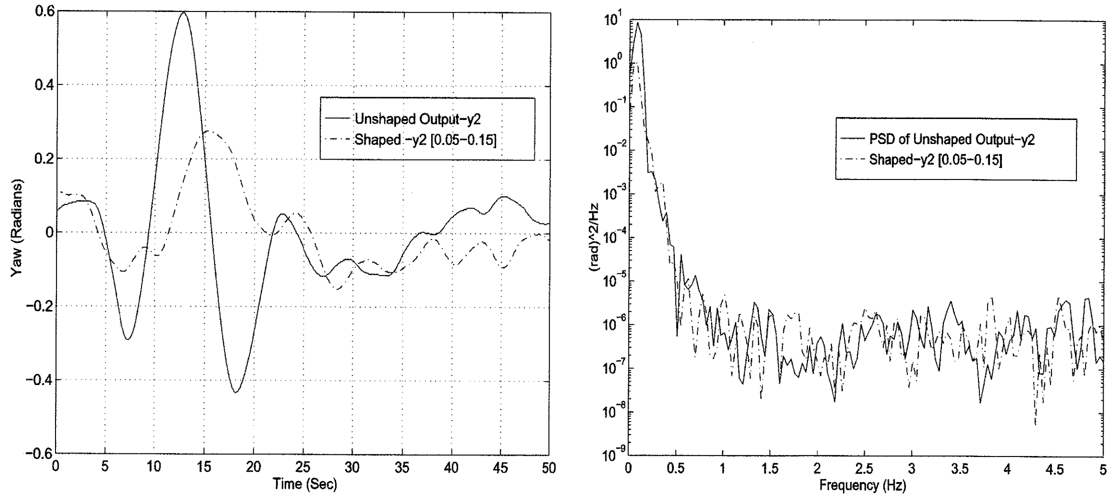

(a) Time domain. (b) Power spectral density.

Fig. 13 Yaw response with a band-stop filtered doublet input, $u_2 \rightarrow y_2$: (a) time domain; (b) power spectral density

7 CONCLUSION

A 2DOF TRMS model whose dynamics resemble that of a helicopter has been successfully identified. The extracted model has been employed for designing and implementing open-loop control.

A feedforward control technique, which is related to a number of approaches known as 'input shaping control', has been investigated. In these methodologies an input signal is shaped so that it does not contain spectral components at the system resonance eigenfrequencies. The study revealed that better performance in attenuation of system vibration at the resonance modes is achieved with low-pass filtered input, as compared with a band-stop filter. This is due to indiscriminate spectral attenuation at frequencies above the cut-off frequency in the low-pass filtered input. However, this is at the expense of a slightly longer move time compared with the band-stop filter.

Open-loop control presents several advantages:

1. It reduces the settling time of the commanded manoeuvre, and hence subsequent command signals can be processed quickly, thereby making the system response fast.
2. Vibrational modes are suppressed, thereby improving the stability characteristics of the system.
3. Feedback controllers for MIMO systems are generally designed for each channel and are decoupled from the other channels. If modal coupling exists, they cannot eliminate vibration caused by the motion in the other channels. However, this type of vibration can be effectively suppressed by shaped reference inputs.

Open-loop control using digital filters forms an important preliminary part of closed-loop control design, in particular for flexible systems such as flexible aircraft/TRMS. This is a topic of future investigation.

ACKNOWLEDGEMENTS

S. M. Ahmad gratefully acknowledges the financial support of the University of Sheffield and the Department of Automatic Control and Systems Engineering. The authors would also like to thank Dr H. A. Thompson, Manager, Rolls-Royce University Technology Centre in Control and Systems Engineering, the University of Sheffield, for many valuable comments on helicopter dynamics.

REFERENCES

1 **Tokhi, M. O.** and **Azad, A. K. M.** Active vibration suppression of flexible manipulator system open-loop control methods. *Int. J. Active Control*, 1995, **1**(1), 15–43.

2 **Poerwanto, H.** Dynamic simulation and control of flexible manipulators systems. PhD thesis, Department of Automatic Control and Systems Engineering, The University of Sheffield, 1998.

3 **Singer, N. C.** and **Seering, W. P.** Preshaping command inputs to reduce system vibration. *Trans. ASME, J. Dynamics Systems, Measmt, and Control*, 1990, **112**(1), 76–81.

4 **Dimitry, G.** and **Vukovich, G.** Nonlinear input shaping control of flexible spacecraft reorientation maneuver. *J. Guidance, Control, and Dynamics*, 1998, **21**(2), 264–269.

5 **Suk, J., Kim, Y.** and **Bang, H.** Experimental evaluation of the torque-shaping method for slew maneuver of flexible space structures. *J. Guidance, Control, and Dynamics*, 1998, **21**(6), 817–822.

6 **Teague, E. H., How, J. P.** and **Parkinson, B. W.** Control of flexible structures using GPS: methods and experimental results. *J. Guidance, Control, and Dynamics*, 1998, **21**(5), 673–683.

7 **Livet, T., Fath, D.** and **Magni, J. F.** Robust flight control design with respect to delays, control efficiencies and flexible modes. *Control Engng Practice*, 1995, **3**(10), 1373–1384.

8 **Livet, T., Fath, D.** and **Kubica, F.** Robust autopilot design for a highly flexible aircraft. In *IFAC'96*, San Francisco, California, 1996, Preprints, Vol. P, pp. 279–284.

9 **George, K. K.** and **Bhat, M. S.** Two-degree-of-freedom H_∞ robust controller for a flexible missile. *J. Guidance, Control, and Dynamics*, 1998, **21**, 518–520.

10 **Waszak, M. R.** and **Schmidt, D. K.** Flight dynamics of aeroelastic vehicles. *J. Aircr.*, 1988, **25**, 263–271.

11 **Meckl, P. H.** and **Seering, W. P.** Experimental evaluation of shaped inputs to reduce vibration of a Cartesian robot. *Trans. ASME, J. Dynamic Systems, Measmt, and Control*, 1990, **112**(6), 159–165.

12 **Dougherty, H., Tompetrini, K., Levinthal, J.** and **Nurre, G.** Space telescope pointing control system. *J. Guidance, Control, and Dynamics*, 1982, **5**(4), 403–409.

13 **Franklin, G. F., Powell, J. D.** and **Emami-Naeini, A.** *Feedback Control of Dynamic Systems*, 1998 (Addison-Wesley, Reading, Massachusetts).

14 **Blight, J. D., Dailey, R. L.** and **Gangsaas, D.** Practical control law design for aircraft using multivariable techniques. In *Advances in Aircraft Flight Control* (Ed. M. B. Tischler), 1996, pp. 231–267 (Taylor and Francis, London).

15 **Ahmad, S. M., Chipperfield, A. J.** and **Tokhi, M. O.** Parametric modelling and dynamic characterization of a two-degree-of-freedom twin rotor multi-input multi-output system. *Proc. Instn Mech. Engrs, Part G: J. Aerospace Engineering*, 2001, **215**(G2), 63–78.

16 **Ahmad, S. M., Chipperfield, A. J.** and **Tokhi, M. O.** Dynamic modelling and control of a 2 dof twin rotor multi-input multi-output system. In Proceedings of IEEE Industrial Electronics, Control and Instrumentation Conference (*IECON'2000*), Nagoya, Japan, 22–28 October 2000, pp. 1451–1456.

17 **Ahmad, S. M., Chipperfield, A. J.** and **Tokhi, M. O.** Dynamic modelling and open loop control of a twin rotor MIMO system. *Proc. Instn Mech. Engrs, Part I: J. Systems and Control Engineering*, 2002, **216**(I6), 477–496.

18 *Twin Rotor MIMO System*, Manual 33-007-0, 1996 (Feedback Instruments Limited, Sussex).
19 **Ahmad, S. M., Chipperfield, A. J.** and **Tokhi, M. O.** Dynamic modelling and linear quadratic Gaussian control of a twin-rotor multi-input multi-output system. *Proc. Instn Mech. Engrs, Part I: J. Systems and Control Engineering*, 2003, **217**(I3), 203–227.
20 **Jackson, L. B.** *Digital Filters and Signal Processing*, 1989 (Kluwer Academic Publishers, London).
21 **Williams, C. S.** *Designing Digital Filters*, 1986 (Prentice-Hall, Englewood Cliffs, New Jersey).
22 **Dwight, H. B.** *Tables and Integrals and Other Mathematical Data*, 3rd edition, 1958 (Macmillan, New York).